# EXPERIMENTS ON WARM PRESTRESS EFFECT AND THEIR NUMERICAL SIMULATION BASED ON LOCAL APPROACH

E. Roos, U. Alsmann, K. Elsässer, U. Eisele and M. Seidenfuss

**Abstract** - A component which is prestressed in the upper shelf of fracture toughness shows nearly the same load bearing capacity when reloaded in the lower shelf; that means a remarkably higher load compared to pure $K_{Ic}$ loading in the lower shelf of fracture toughness. This well-known effect is called the warm preststress (WPS) effect. In the paper experimental results for different load cycles will be presented. The influence of specimen size on the WPS effect is demonstrated. Experiments with the purpose of separating the mechanisms of WPS are presented. For the numerical description of the phases of the WPS effect the Rousselier model (upper shelf) and the Beremin model (lower shelf) are choosen. Different loading pathes are simulated numerically, investigating stress states in comparison with $K_{Ic}$ specimen. Fracture load after WPS is predicted by local approach.

## Introduction

Warm prestressing (WPS) consists of initially loading a cracked specimen or component at a temperature above the brittle-to-ductile transition region and yields to a remarkably higher load compared to pure $K_{Ic}$ loading when reloaded in the lower shelf of fracture toughness. This well known beneficial effect of WPS has been extensively reported in literature, e.g. /1/. It is also known, /2/, that this effect results from the three mechanisms blunting of the crack tip, favorable stress distribution compared to pure $K_{Ic}$ loading and highly prestrained material around the crack tip. In order to investigate the mechanisms of WPS and to simulate the effect by means of local approach models different load cycles for different specimen sizes have been examined. The material investigated and presented in the paper is the highly tough shape welded steel 10 MnMoNi 5 5. This steel shows a Charpy energy level of around 200 J in the upper shelf and a $RT_{NDT}$ of -45°C. Figure 1 shows the corresponding scatterband of fracture toughness ($K_{Ic}$ and $K_{Ji}$ values) and the load cycles LCF (Load-Cool-Fracture) and LUCF (Load-Unload-Cool-Fracture).

## Experimental results of WPS-simulation

For both load cycles, LCF and LUCF, the temperature of warm prestressing $T_{WPS}$ was chosen to be at the beginning of the upper shelf of fracture toughness, which means 30°C for the presented material, /3/. The level of warm prestressing was chosen to be close to ductile crack initiation, for the presented material at $J_i$ = 125 N/mm. The temperature $T_{FRAC}$ at which fracture load was applied was chosen to be in the lower shelf of fracture toughness, for the presented material at -150°C.
To present the experimental results, both, the preload and fracture load is expressed in $K_I$. The stress intensity factor $K_I$ is based on elastic loads only. In case of large plastic

MPA Staatliche Materialprüfungsanstalt, University of Stuttgart
Paffenwaldring 32, 70569 Stuttgart, Germany

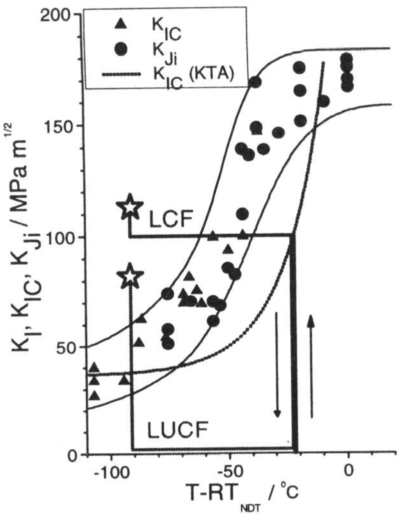


Fig. 1: Load cycles LCF and LUCF

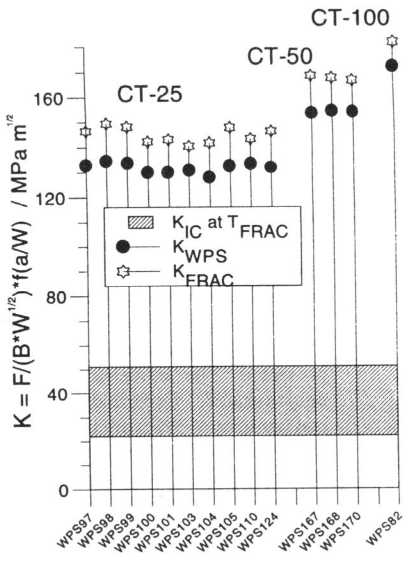


Fig. 2: Experimental results LCF load cycle

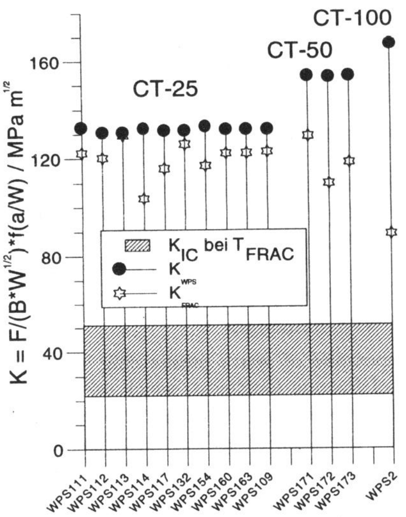


Fig. 3: Experimental results LUCF load cycle

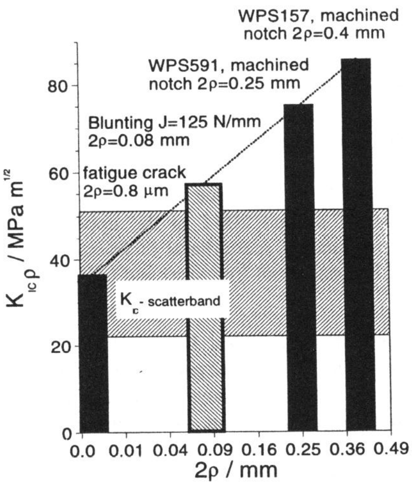


Fig. 4: Influence of crack tip blunting on $K_{Ic(\rho)}$ at -150°C

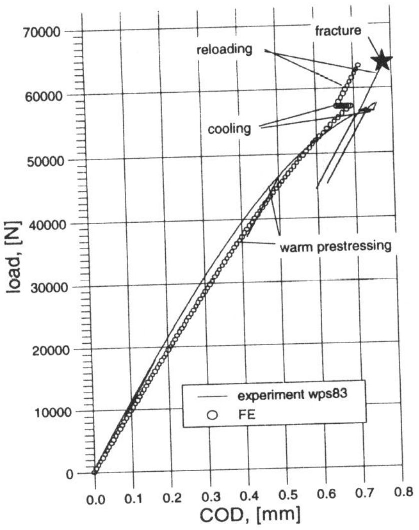


Fig 5: Load deformation behaviour LCF

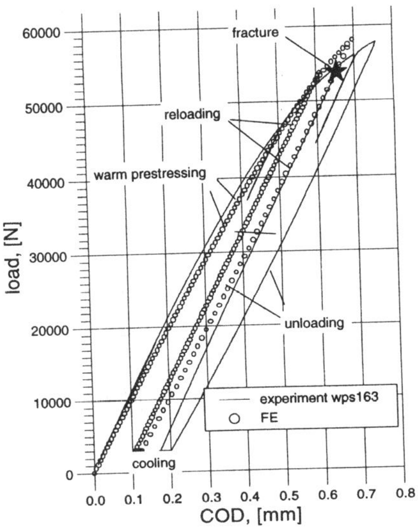


Fig. 6: Load deformation behaviour LUCF

deformations this is not an adaequate parameter to describe the crack tip stress field, nevertheless $K_I$ still is a direct measure of the applied load of the specimen.
Figures 2 and 3 ,/3/, summarize the results of the experimental WPS-simulations of LCF and LUCF load cycles:
In the case of the LCF cycle fracture load for all tested geometries reaches the level of preload. The additional increase in load ($K_{FRAC}$ - $K_{WPS}$) at fracture is, independent of examined geometry, around 10 MPam$^{1/2}$. Compared to $K_{Ic}$ values of non warm prestressed specimen this means an increase of the apparent fracture toughness of 380%-490%. Compared to the scatter band of $K_{Ic}$ - values of the examined material the fracture loads after LCF cycle show very little scatter.
In the case of the LUCF cycle fracture load does not reach the level of preload in any case. Larger scatter is observed compared to the LCF results. Additionally, for the LUCF cycle of the examined material a scale effect can be observed:
The ratio $K_{FRAC}/K_{WPS}$ reaches a maximum value of about 90% in the case of 20% sidegrooved CT-25 specimen compared to 53% in the case of 20% sidegrooved CT-100 specimen. Compared to $K_{Ic}$ values of non warm prestressed specimen this means an increase of the apparent fracture toughness of around 350% (CT-25) to 250% (CT-100).

In order to separate the influences on the WPS effect, crack tip blunting has been examined by performing $K_{Ic}$ tests with CT specimens with machined notches, /3/. Crack tip blunting after warm prestressing at J=125N/mm has been determined in metallographic cuts. As this crack tip blunting couldn't be reproduced exactly by a machined notch, specimens with two different notch radii have been tested and the results have been extrapolated to the crack tip blunting by means of the proportionality between $K_{Ic(\rho)}$ and $\rho^{1/2}$ given in /4/. Figure 4 shows that this yields to fracture toughness values of 55-60 MPam$^{1/2}$ for a CT-25 specimen

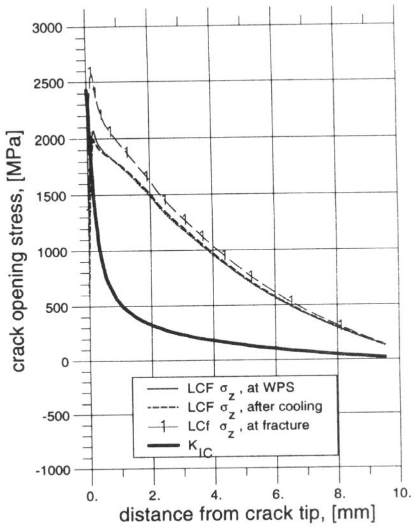


Fig. 7: Stress distributions for the LCF cycle

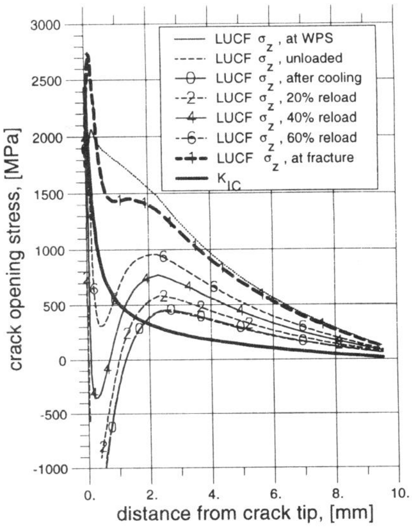


Fig. 8: Stress distributions for the LUCF cycle

with a machined notch corresponding to the measured crack tip blunting. These values compared to $K_{Ic}$ values of fatigue cracked CT specimens on the one hand ($K_{Ic}$ = 22-51 $MPam^{1/2}$) and $K_{FRAC}$ values at fracture after LUCF on the other hand ($K_{FRAC}$ = 100-129 $MPam^{1/2}$ ) show that the increase of apparent fracture toughness due to the geometric effect of crack tip blunting is not the major contribution to the WPS effect.

## Numerical simulation of WPS load cycles

Taking crack tip blunting, isotropic hardening and thermal expansion during the cooling phase into account, /5/, the load-deformation behaviour of LCF and LUCF load cycles have been simulated using the Finite Element Method, figures 5 and 6. Experimentally and numerically determined load-deformation behaviour are in good agreement.

The evolution of the opening stress during the LCF cycle in comparison with stress distributions for $K_{Ic}$ are shown in figures 7 and 8 . It can be observed that:

-In case of WPS cycles due to plastic deformation at WPS a greater part of the ligament is exposed to a high stress level at fracture compared to the $K_{Ic}$ distribution. The high stress level in the ligament corresponds qualitatively to the higher load at fracture.

-The maximum of the stress distribution near the crack tip at fracture is comparable for all three cases shown.

-Cooling at constant load doesn't affect the stress distribution significantly.

In order to predict specimen or component failure in the different phases of WPS cycles two local approach models have been choosen:

1. The Rousselier model to describe crack initiation and crack growth in the upper shelf region of fracture toughness, /6/.
2. The Beremin model to describe cleavage fracture in the lower shelf region of fracture

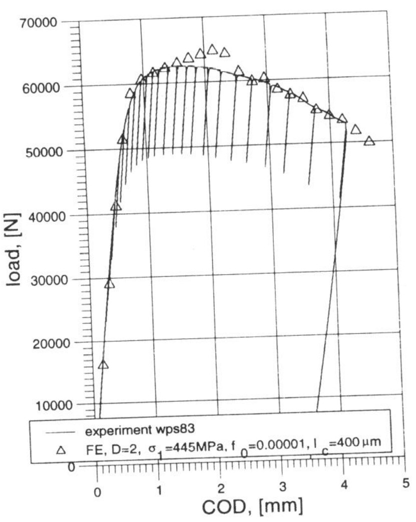


Fig. 9: Load-deformation behaviour in the upper shelf

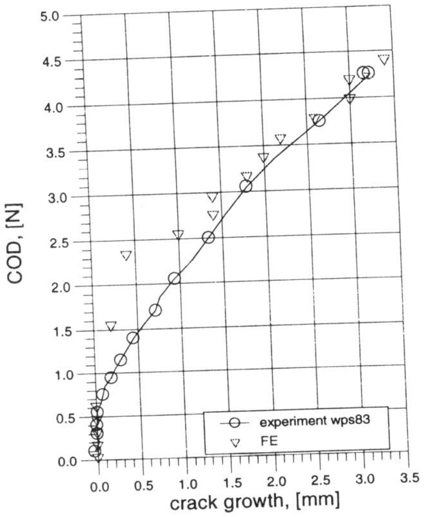


Fig. 10: Crack growth in the upper shelf

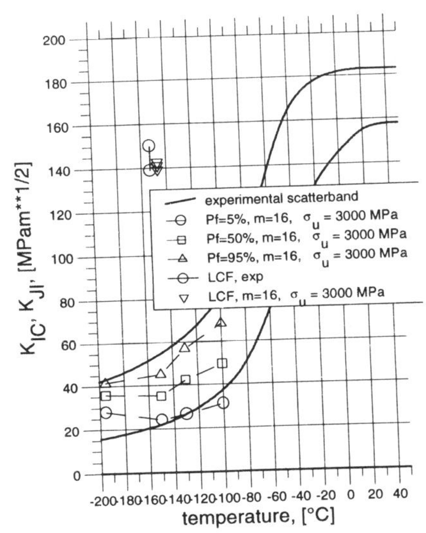


Fig. 11: Experimentally and numerically determined fracture loads, LCF

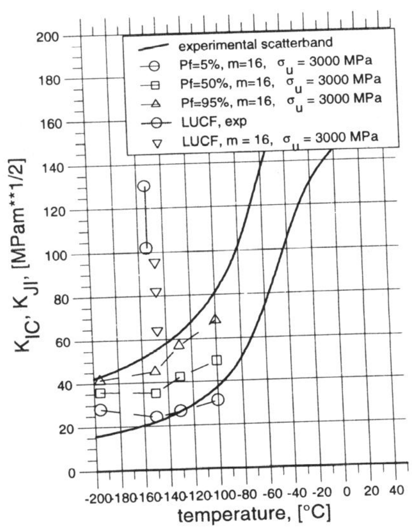


Fig. 12: Experimentally and numerically determined fracture loads, LUCF

toughness, /7/.

As shown in figures 9 and 10, using the Rousselier model it is possible to predict well specimen behaviour in the upper shelf of fracture toughness including crack initiation and crack growth, /8/. To predict fracture loads in the lower shelf after WPS cycles LCF and LUCF the Beremin model was employed. Figures 11and 12 shows the predictions for both load cycles, taking into account only the active plastic zone and having fixed the model parameters to the experimental $K_{Ic}$ scatterband, since the Weibull parameters determined from round notched tensile bars are not transferable to fracture mechanics specimens, /5/. As it can be observed, the fracture load is well predicted in the case of the LCF cycle and somewhat underestimated in the case of LUCF cycle.

## Summary

For the presented material it has been demonstrated that:

- In the case of LCF cycle fracture load has always been higher than preload, whereas in the case of LUCF cycle fracture load does not attain the preload level.
- The beneficial effect of warm prestressing results mainly from a favorable stress distribution, whereas the contribution of crack tip blunting is less important.
- Crack initiation and crack growth can be simulated qantitatively by Rousselier's model.
- Using the Beremin model failure load is predicted quantitatively in the case of LCF cycle and underestimated in the case of LUCF cycle. The model parameters are found to be not transferable from notched to cracked specimen.

## Acknowledgements

The presented work was sponsored by the Bundesministerium für Bildung und Forschung (BMBF) and the Vereinigung der Großkraftwerksbetreiber (VGB).

## Literature

/1/ Smith, D. J. and S. J. Garwood; The Significance of Prior Overload on Fracture Resistance: A Critical Review; Int. J. Pres. Ves. & Piping 41 (1990), pp 255-296

/2/ Beremin, F. M.; Numerical Modelling of Warm Prestress Effect using a Damage function for cleavage fracture; Proc. ICF5, Pergamon Press Oxford, 1981, Vol .2, pp 825-832

/3/ Roos, E. and U. Alsmann; Experimentelle Untersuchungen zu den Mechanismen des WPS-Effekt; 23. MPA Seminar 1997, MPA Universität Stuttgart, Vol. 1, pp 24.1-24.21

/4/ Wilshaw, T. R., C. A. Rau and A. S. Tetelman, A General Model to predict the elastic-plastic Stress Distribution and Fracture, Strength of Notched Bars in Plane Strain Bending

/5/ Roos, E. and K. Elsäßer; Experimentelle und numerische Untersuchungen zur Anwendbarkeit von Local Approach Ansätzen auf den WPS Effekt; 23. MPA Seminar 1997, MPA Universität Stuttgart, Vol. 2, pp 26.1-26.19

/6/ Rousselier, G.; Ductile Fracture Models and their Potential in Local Approach of Fracture; Nuclear Engineering and Design 105, 1987, pp. 97-111

/7/ Beremin, F. M.; A Local Criterion for Cleavage Fracture of a Nuclear Pressure Vessel Steel; Metallurgical Transactions A, Vol. 14A, November 1983, pp. 2277-2287

/8/ Eisele, U., M. Seidenfuß and J.-M. Pitard-Bouet; Comparison Between Fracture Mechanics and Local Approach Models for the Analysis of Shallow Cracks; Journal de Physique IV, Vol. 6, octobre 1996, pp. C6-75 - C6-89.